EXAFS and IR Analysis of Electrochromic NiO$_x$/NiO$_x$H$_y$ Thin Films

Jana Padežnik Gomilšek,[1] Romana Cerc Korošec,[2] Peter Bukovec[2] and Alojz Kodre[3,4]

[1] *Faculty for Mechanical Engineering, Smetanova 17, SI-2000 Maribor, Slovenia*

[2] *Faculty of Chemistry and Chemical Technology, Aškerčeva 5, SI-1000 Ljubljana, Slovenia*

[3] *Faculty of Mathematics and Physics, Jadranska 19, SI-1000 Ljubljana, Slovenia*

[4] *Jožef Stefan Institute, Jamova 39, SI-1000 Ljubljana, Slovenia*

* Corresponding author: E-mail: jana.padeznik @uni-mb.si

Abstract

Electrochromic (EC) thin films of NiO$_x$ and NiO$_x$H$_y$ are prepared by sol-gel method from nickel chloride precursor and deposited onto a suitable substrate by dip-coating technique. The development of the structure with thermal treatment is investigated by EXAFS and IR spectroscopy in two series of films, with high and low concentration of chloride as counter ions. In the former, the predominant structure before thermal treatment is nickel hydroxide. The baking induces condensation, yet with no trace of NiO. In the latter group, colloidal particles are indicated, on which acetate groups are adsorbed or coordinated. At the maximum EC-response the formation of NiO grains is established by EXAFS and IR.

Keywords: Electrochromism, thin films, nickel oxide, nickel hydroxide, EXAFS

1. Introduction

Electrochromic (EC) nickel oxide/hydroxide thin films are good candidates for ion-storage materials in combination with tungsten oxide in complementary electrochromic devices.[1] Under anodic potentials they change colour from transparent to deep brown. Chemically prepared thin films are amorphous after the deposition process. They have to be thermally treated in order to adopt a stabilised structure ensuring a large number of switch cycles from a coloured to a bleached state and vice-versa. The magnitude of the optical modulation and stability of the film structure depend critically on the thermal treatment,[2–6] but there is no explicit rule for the extent of the treatment to obtain optimum properties. For sol-gel prepared electrochromic thin films the counter-ions (sulfates, acetates etc.) play an active role in the formation of the structure and in the mechanism of the coloration during the cycling process.[7]

Although the choice of experimental techniques to monitor the structural morphological evolution of the films is limited due to the very small sample mass, it is essential to study the films themselves since they behave differently from corresponding powders.[8,9] For films prepared from nickel sulfate and nickel acetate precursor and with varying extent of thermal treatement,[7] EXAFS (Extended X-ray Absorption Fine Structure) analysis performed ex-situ has proved to be a powerful tool to study local atomic structural changes. Another amenable tool is IR (Infra-Red) spectroscopy whereby the structural changes which occur during heating can be followed through the fingerprints of characteristic vibrations.

Nickel chloride is often used as a precursor salt for the preparation of electrochromic NiO films.[10–13] It is highly soluble in water as well as in alcohol media.

In this work, two series of sol-gel prepared thin films from nickel chloride precursor with different concentration of counter ions are studied: by washing the sol the content of chloride counter ions is greatly reduced and the relative amount of acetate counter ions is enhanced.

The films deposited on a suitable substrate are analyzed by EXAFS and IR spectroscopy at different

Table I. List of samples.

No		Heat treatment		Degree of thermal decomposition of acetate groups / %	Coloration efficiency of 101st cycle at λ = 480 nm/cm^2 C^{-1}
1A	unwashed sol	30 min	200 °C	7	–63*
1B		45 min		13	–52
1C		60 min		18	–45
2A	washed sol	18 min	230 °C	10	–33
2B		26 min		15	–41
2C		33 min		20	–42

* bleaching process is not reversible i.e. at the end of the cycle transmittance of the film does not reach its value of the beginning of the cycle. This is characteristic behavior for films which were not enough thermally treated.[8,9]

steps of the heat treatment, close to that of optimum EC response determined in previous tests[14]. Optimum EC response is a compromise between change in transmittance from the bleached to the coloured state and the reversibility of the process: lower temperature and shorter duration lead to non-reversibility of the bleaching process in both types of films whereas higher temperature of the heat-treatment and longer duration to poorer electrochromic effect. In our study, the duration of the heat treatment at optimum temperatures of 200 °C and 230 °C for unwashed and washed samples, respectively, is varied. The maximal colouration efficiencies in the stabilized 100th cycle are achieved after, respectively, 45 and 33 min. Some more details on sample properties are given in Table I.

2. Experimental

2.0 M LiOH solution was added dropwise to 0.6 M solution of nickel(II) chloride to pH 9.0. For one series of samples, the green precipitate was washed four times with water. For both series, the slurry was peptised with glacial acetic acid to pH 4.5, some water was added to adjust the viscosity. For unwashed samples the green precipitate was only centrifuged so that a high amount of chloride and lithium ions was retained (11.6 wt. % Cl$^-$ and 1.58 wt. % Li$^+$ vs 1.9 wt. % Cl$^-$ and $3 \cdot 10^{-3}$ wt. % Li$^+$ in washed samples). Consequently, the acetate content is somewhat higher in washed samples (48.2% vs. 39.6%).

Chloride and acetate contents in the samples were determined by ion chromatography (IC) and the lithium concentration was determined by flame atomic absorption technique (AAS).

Thin-film samples are deposited on the support with dip coating technique. The thickness is too low to be determined with profilometry, which means that sample thickness is lower than 40 nm. The samples for EXAFS and IR measurements are heat treated in muffle furnace (Bosio, Slovenia) allowing the temperature accuracy of ± 1 C. The degree of thermal decomposition of acetate groups is calculated from isothermal TG measurements

(Mettler Toledo TG/SDTA 851^e Instrument) of the films, deposited on Pt foil.[8,9,14]

Thin-film samples for EXAFS analysis were deposited on Al foil to reduce x-ray absorption in the support material and to improve the signal-to-background ratio. Even so, only 12–15 layers of films could be superposed, limiting the absorption jump at Ni K edge to ~0.1. Standard Ni K-edge EXAFS spectra were recorded at the E4 beamline of the synchrotron laboratory Hasylab at DESY, Hamburg, Germany, using a Si(111) double-crystal monochromator with energy resolution of ~1 eV at the Ni K edge (8332 eV). Higher harmonics were efficiently removed by a slight detuning of the crystals. The x-ray flux was measured by three ionization detectors filled with 100, 600 and 1000 mbar of Ar, respectively. The samples were inserted between the first pair, and Ni metal foil for energy calibration between the second pair of the detectors. The measured EXAFS spectra are analyzed with IFFEFIT code.[15,16]

Fourier-transform infrared (FT-IR) spectroscopic measurements are performed on a Perkin-Elmer system 2000 spectrophotometer with a resolution of 4 cm^{-1}. To obtain transverse optical (TO) modes, the films were deposited on Si wafers.

3. Results and Discussion

EXAFS signal is the result of scattering of the outgoing photoelectron along a path visiting neighbor atoms. Each scattering path contributes a periodical component. Its period depends on the length of the path *i.e.* distance to the neighbors, and its amplitude is proportional to the number of neighbors on equivalent paths. The shape of the signal envelope is correlated to the atomic species and the degree of order in the structure. Fourier transform of the EXAFS signal separates the contributions of the consecutive shells of neighbors into a series of peaks in the order of increasing distances. In the fitting process the quantitative structural information is extracted from EXAFS signal by comparison to the artificial signal constructed from a model array of atoms. For each shell of neighbors its set of characteristic parameters is relaxed toward best agreement between the model and the measured signal.

Fourier transforms (FT) of the Ni EXAFS spectra are shown in Fig. 1. They differ in the height and position of the second peak: its rise with temperature is rapid in the washed sample and gradual in the unwashed sample, where its position is shifted for ~0.10 Å. The small absorbance of the samples with the consequent high noise level of the spectra limits the scope of the structural analysis. The useful *k*-range reaches only up to 10–12 Å^{-1}. This is only sufficient to detect changes in the closest two neighbor shells due to preparation procedure and the degree of heat treatment.

EXAFS model of the Ni atom neighborhood, encompassing the region of the first two peaks in the Fourier transforms (1 Å–3 Å), is built on the basis of NiO bunsenite structure[17] with an octahedron of 6 O neighbors in the first shell and 12 Ni neighbors in the second one with bond distances 2.09 Å and 2.95 Å, respectively. The model gives, after moderate changes of Ni–O and Ni–Ni distances and a large reduction in the number of the second-shell neighbors, a good agreement with measured data for washed samples and a moderate one for unwashed samples. In the latter, the fit is improved by addition of ~1 Cl neighbor at 3.33 Å. A further improvement with some C atoms from organic groups (presumably nickel acetate) beyond the first shell is inconclusive due to high correlation of parameters.
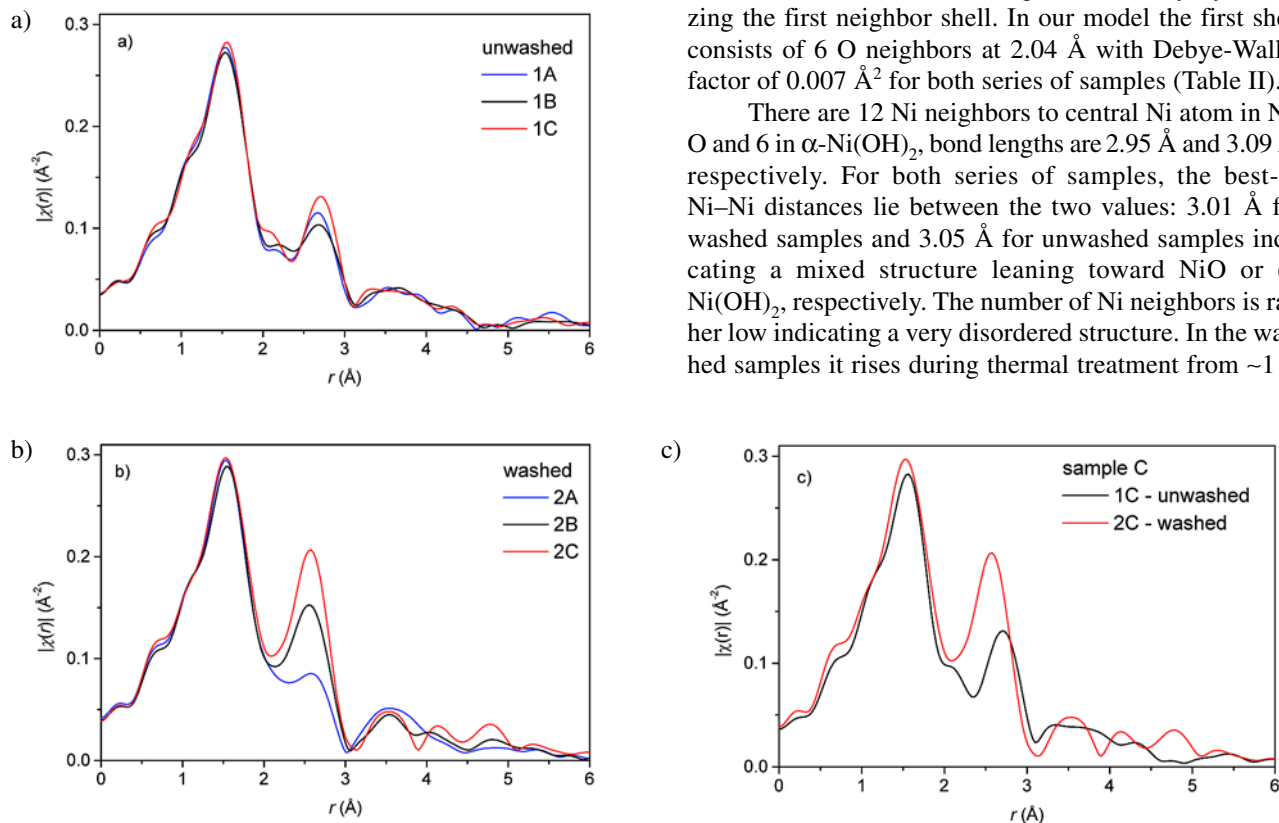
To remove the correlation between the coordination numbers and the Debye-Waller factors, the latter are fixed at some value acceptable for the entire series, so that the former can be reliably determined. In the first shell, however, full occupation of oxygen octahedron is presumed and the Debye-Waller factor is varied. As usual in EXAFS analysis, the most reliably determined parameters are the interatomic distances.

On the hint from IR results as discussed below, the leading scattering paths from the α-Ni(OH)$_2$ structure are examined for inclusion into the model. The exact structure of α-Ni(OH)$_2$ is still an open question.[18] It is suggested that the first shells of neighbors in α-Ni(OH)$_2$ are similar to ordinary brucite β-Ni(OH)$_2$: a distorted octahedron of 6 OH groups in the first shell and 6 Ni neighbors in the second one, with bond distances of 2.12 Å and 3.13 Å, respectively.[19] In contrast to β-Ni(OH)$_2$, the layers of Ni–OH octahedra in α-Ni(OH)$_2$ are intercalated with water molecules expanding the c-axis from 4.6 Å to about 8 Å. Simultaneously, a contraction of lattice within the plane of the layer is reported[20] yielding Ni–O and Ni–Ni bond distances of 2.05 Å and 3.09 Å, respectively.

The first neighbor shell is almost identical in NiO and α-Ni(OH)$_2$: it comprises the oxygen octahedron around Ni atom, with Ni–O bond length of 2.09 Å or 2.05 Å, respectively. In disordered films a reduction of the length relative to the NiO perfect-crystal value is expected, so the structures cannot be distinguished merely by analyzing the first neighbor shell. In our model the first shell consists of 6 O neighbors at 2.04 Å with Debye-Waller factor of 0.007 Å^2 for both series of samples (Table II).

There are 12 Ni neighbors to central Ni atom in NiO and 6 in α-Ni(OH)$_2$, bond lengths are 2.95 Å and 3.09 Å, respectively. For both series of samples, the best-fit Ni–Ni distances lie between the two values: 3.01 Å for washed samples and 3.05 Å for unwashed samples indicating a mixed structure leaning toward NiO or α-Ni(OH)$_2$, respectively. The number of Ni neighbors is rather low indicating a very disordered structure. In the washed samples it rises during thermal treatment from ~1 to
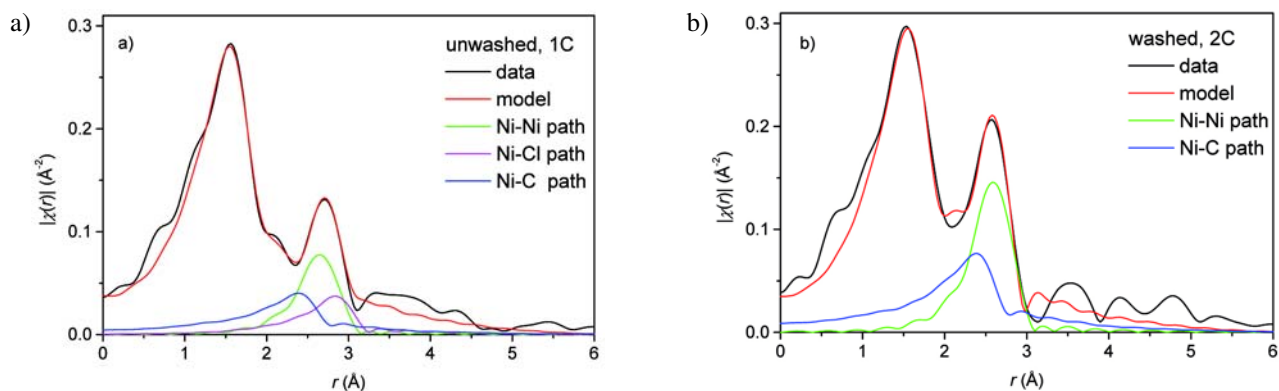

a)

b)

c)

Figure 1. EXAFS spectra of thin films (weighing k^1, Hanning window, k = 3 ..12 Å^{-1}, dk = 1 Å^{-1}). a) series 1, b) series 2, c) the effect of washing.

a)

b)

Figure 2. EXAFS spectra and their models. Structural components of the second peak model are also shown. a) sample 1C, b) sample 2C (weighing k^1, Hanning window, $k = 3 .. 12$ Å^{-1}, dk = 1 Å^{-1}).

~4, reflecting the gradual crystallization, the high value still being well below half of the ideal crystal occupancy. The fit improves by addition of C neighbors at ~2.90 Å, but the parameters are highly correlated, with large error brackets. The best fit numbers follow approximately the number of Ni. In the unwashed samples the second peak in FT is resolved into contributions of Ni and Cl neighbors, again highly correlated. Structural changes induced by heat treatment are less profound and the total number is lower than in the washed samples: ~1 Cl and ~2 Ni neighbors are found by fit. The number of chlorine neighbors cannot be interpreted in terms of stoichiometry since chlorine is not directly coordinated to Ni ions but occupies the third shell of neighbors, outside the oxygen envelope.

In the IR spectra of thermally untreated samples of the first series (Fig. 3A) the presence of layered α-$Ni(OH)_2$ structure[21] is indicated by stretching ν(O–H) vibrations, shifted towards higher wavenumbers (3600 cm^{-1}) due to non-hydrogen bonded O–H groups and by the band positioned at 673 cm^{-1} corresponding to in-plane δ(Ni–OH) deformation[21] – see Table III. The difference between asymmetric and symmetric vibrations of the acetate groups is 150 cm^{-1}. Acetate groups originate from peptizing agent (acetic acid) and play an active role in the formation of the structure. From this difference (Δν) the type of coordination of the acetate groups to the metal ions can be deduced.[22] In the bridging complex Δν is practically the same as with free ion. We can therefore suppose that acetate groups are located between the $Ni(OH)_2$ slabs or bridge-bonded to nickel cations.

During heat treatment the signal of acetate groups diminishes due to thermal decomposition. A small peak, probably corresponding to a hydrogen bonded O–H stretching, appears at 3389 cm^{-1}. In spectra of the second series with very low concentration of chloride, this peak is absent, indicating that it corresponds to O–H····Cl stretching. In our tentative picture the counter ions (chlorides) are present between the α-$Ni(OH)_2$ slabs. With thermal decomposition of acetates the layers come closer together enhancing interaction between hydroxide groups and chloride anions. The shoulder at 1626 cm^{-1} indicates some acetate groups with monodentate coordination.

IR spectra of the second series (Fig. 3B) show no $Ni(OH)_2$ formation, pointing to adsorption or coordination of acetate groups on the colloidal particles. The small peak at 415 cm^{-1} in the spectrum of the 2C sample indicates the beginning of the NiO formation.

Table II. Model parameters. $r = 1.2–3$ Å, $dr = 0.1$ Å, $k = 3–12$ Å^{-1}, $dk = 0.1$ Å^{-1}, weighing k^1, $E_0 = -5(1)$ eV, $S_0^2 = 0.83$. The goodnes of the fit (r_{fit}) is between 0.001 and 0.003 for all models. Uncertainties of the last digit are given in parentheses; if absent the parameter is kept fixed.

sample	path	N	r [Å]	σ² [Å²]
1A	Ni–O	6	2.03(1)	0.007(1)
	Ni–C	1.3(9)	2.90	0.003
	Ni–Ni	1.7(6)	3.04(1)	0.005
	Ni–Cl	1.0(3)	3.33(5)	0.003
1B	Ni–O	6	2.04(1)	0.007(1)
	Ni–C	1.5(9)	2.90	0.003
	Ni–Ni	1.2(6)	3.04(2)	0.005
	Ni–Cl	1.2(4)	3.33(4)	0.003
1C	Ni–O	6	2.04(1)	0.007(1)
	Ni–C	2.0(9)	2.90	0.003
	Ni–Ni	2.1(7)	3.06(1)	0.005
	Ni–Cl	1.0(4)	2.33(1)	0.003
2A	Ni–O	6	2.03(2)	0.006(1)
	Ni–C	1.3(5)	2.90	0.003
	Ni–Ni	1.1(2)	3.03(2)	0.005
2B	Ni–O	6	2.04(1)	0.007(1)
	Ni–C	2.9(6)	2.90	0.003
	Ni–Ni	2.6(3)	3.01(1)	0.005
2C	Ni–O	6	2.04(1)	0.007(1)
	Ni–C	3.8(3)	2.90	0.003
	Ni–Ni	3.7(3)	3.00(1)	0.005

Table III: Functional groups and observed wavenumbers of both series of samples.

Observed vawenumber, cm⁻¹ First series	Observed vawenumber, cm⁻¹ Second series	Functional group
3400 (broad)	3400 (broad)	OH stretch
1578	1565	Asymmetric stretch of acetate (COO⁻)
1428	1421	Symmetric stretch of acetate (COO⁻)
	1345	CH_3 deformation
1051, 1024	1049, 1028	CH_3 rocking
	677	OCO deformation
673		OH in-plane deformation
	618	OCO and CH out-of-plane bending
~400	~400	NiO stretch

a)

b)
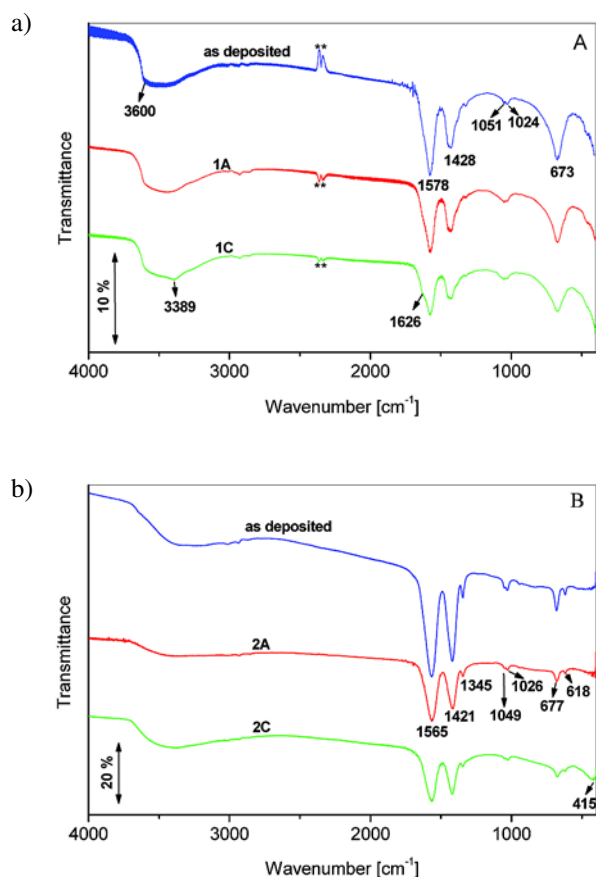
Figure 3. IR transmittance spectra of both types of samples, a) unwashed, b) washed. ** indicates CO_2 absorption due to insufficient purging.

4. Conclusions

The presence of chlorine counter ions in electrochromic thin films leads to the formation of different structure and lowers the temperature of optimum heat treatment in comparison to films containing only acetate counter ions.

In EXAFS spectra of the films, the unchanging amplitude of the first FT peak points to the constant oxygen octahedron of the Ni atom. The degree of crystal order is reflected in the amplitude of the second peak in the Fourier transforms. In the washed samples, gradual crystal grain growth is observed in consecutive steps of heating, reaching one third of the bulk NiO crystal occupancy. In unwashed samples, the chloride ions comprise the third neighbor shell, not directly coordinated to Ni ions. The presence of α-Ni(OH)$_2$ structure is indicated by the increase in the average Ni–Ni distance.

For the washed sample, the optimum response is obtained at approximately the same treatment step as in the nickel acetate precursor; i.e. at 25% decomposition of acetate groups,[7] with grains of nickel oxide already formed inside the amorphous structure.

The unwashed sample shows α-Ni(OH)$_2$ structure and requires less heating for the maximal electrochromic response: it is found at 13% acetate decomposition.[14] By that mark, and even up to 18% decomposition, no formation of NiO structure is indicated by EXAFS, while in the IR spectra only the increase in the condensation degree of the layered structure is observed.

5. Acknowledgement

6. References

1. A. Azens, C. G. Granqvist, *J. Solid State Electrochem.* **2003**, *7*, 64–68.
2. Z. Xuping, C. Guoping, *Thin Solid Films* **1997**, *298*, 53–56.
3. A. Šurca, B. Orel, B. Pihlar, P. Bukovec, *J. Electroanal. Chem.* **1996**, *408*, 83–100.

4. X. Chen, X. Hu, J. Feng, *Nanostruct. Mater.* **1995**, *6,* 309–312.

5. M. Chigane, M. Ishikawa, *J. Electrochem. Soc.* **1994**, *141*, 3439–3443.

6. C. Natarajan, H. Matsumoto, G. Nogami, *J. Electrochem. Soc.* **1997**, *114*, 121–126.

7. R. Cerc Korošec, P. Bukovec, *Acta Chim. Slov.* **2006**, *53*, 136–147.

8. R. Cerc Korošec, P. Bukovec, B. Pihlar, J. Padežnik Gomilšek, *Thermochim. Acta* **2003**, *402*, 57–67.

9. R. Cerc Korošec, P. Bukovec, *Thermochim. Acta* **2004**, *410*, 65–71.

10. L. D. Kadam, P. S. Patil, *Sol. Energy Mater. Sol. Cells* **2001**, *69*, 361–369.

11. P. S. Patil, L. D. Kadam, *Appl. Surf. Sci.* **2002**, *199*, 211–221.

12. W. L. Chao, M. Fan-Li, S. Yu-Feng, H. Xing-Jiu, L. Jin-Hu-ai, *Journal of Inorganic Materials* **2004**, *19*, 1391–1396.

13. W. Xing, F. Li, Z. Yan, G. Q. Lu, *J. Power Sources* **2004**, *134*, 324–330.

14. M. Felicijan, Diploma work, University of Ljubljana, Slovenia, **2005**.

15. B. Ravel, M. Newville*, J. Synchrotron Rad.* **2005**, *12*, 537–541.

16. J. J. Rehr, J. Mustre de Leon, S. I. Zabinsky, R.C. Albers, *J. Am. Chem. Soc.* **1991**, *113,* 5135–5140.

17. R. W. G. Wyckoff, in: Crystal Structures, Second edition, Interscience Publishers, New York, **1963**, p.p. 85 237.

18. J. McBreen, Nickel hidroxides, in: Handbook of battery materials, editor J. O. Besenhard, Wiley-VCH, New York, **1999**.

19. R. W. G. Wyckoff, in: Crystal Structures, Second edition, Interscience Publishers, New York **1963**, p.p. 239 444.

20. M. Balasubramanian, C. A. Melendres, *J. Phys. Chem. B* **2000**, *104*, 4300–4306.

21. P. Oliva, J. Leonardi, J. F. Laurent, C. Delmas, J. J. Braconnier, M. Figlarz, F. Filvet, *J. Power Sources* **1982**, *8*, 229–255.

22. K. Nakamoto, in: Infrared and Raman spectra of Inorganic and Coordination Compounds, 5th Ed., John Wiley & Sons, New York, **1997**.

Povzetek

Elektrokromne tanke plasti NiO_x in NiO_xH_y smo pripravili z metodo sol-gel iz nikelj-kloridnega prekurzorja in jih s tehniko potapljanja nanesli na ustrezno podlago. Razvoj strukture s temperaturo obdelave smo spremljali s spektroskopijama EXAFS in IR pri dveh serijah filmov z visoko oz. nizko koncentracijo kloridnih proti-ionov. V prvi pred termično obdelavo prevladuje struktura nikljevega hidroksida. Segrevanje nato izzove kondenzacijo, vendar brez sledov NiO. V drugi seriji so prisotni koloidni delci, na katere so adsorbirane acetatne skupine. Z obema spektroskopskima metodama smo pri plasteh z največjim elektrokromnim odzivom ugotovili prisotnost strukture nikljevega oksida.